WORKING PAPER

Optimal Timing of Carbon-Capture Retrofit on a Mature Offshore Gas Platform under Stochastic EU-ETS Prices and a Stochastic Decommissioning Deadline

A real-options analysis with a free-boundary HJB and a closed-form perpetual benchmark

O. Vestergaard
T. Brekke

07-MAY-2024

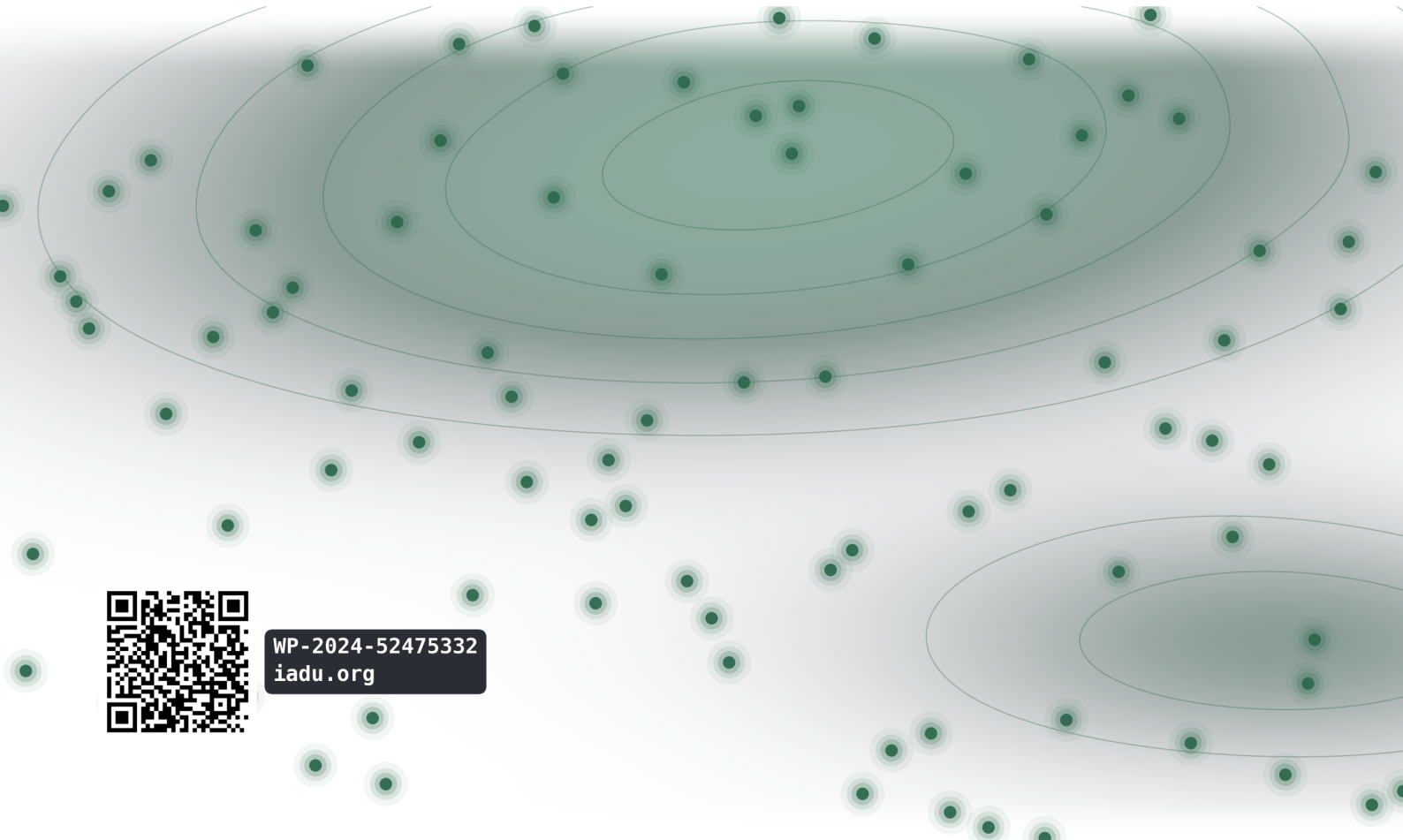

WP-2024-52475332
iadu.org

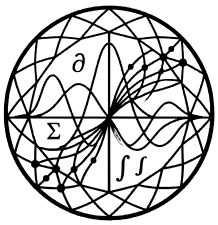

IADU
INSTITUTE FOR
ADVANCED DYNAMIC
UNCERTAINTY

Copyright

Suggested Citation

O. Vestergaard and T. Brekke (2024). 'Optimal Timing of Carbon-Capture Retrofit on a Mature Offshore Gas Platform under Stochastic EU-ETS Prices and a Stochastic Decommissioning Deadline.' *IADU Working Paper* **WP-2024-52475332**.
Available at `https://iadu.org/research/WP-2024-52475332/`.

About IADU

The **Institute for Advanced Dynamic Uncertainty** exists to advance the mathematical theory of decision under uncertainty and to bring that theory, with rigour and restraint, to bear upon the most consequential questions of public and institutional policy. Its work proceeds from the foundations upward: the question shall dictate the method, and never the converse.

Research is organised across five operational divisions: the *Division of Stochastic Analysis and Control*; the *Division of Games, Dynamics, and Strategic Control*; the *Division of Financial Mathematics and Asset Pricing*; the *Division of Quantitative Policy and Macroeconomics*; and the *Division of Sustainability and Energy Economics*. The Institute publishes working papers, technical notes, discussion papers, policy briefs, research and technical reports, preprints, surveys, data reports, and research memoranda, and produces the *IADU Quantitative Policy Review* as its principal vehicle for engagement with the policy community.

The Institute's research is purely bottom-up. It does not begin from a conclusion and retrofit mathematics in its service, nor employ mathematical methods to confirm the prior commitments, the convenience of clients, or the points of view of policymakers, however eminent. The mathematics, not preference, determines what is optimal. The Institute conducts no advocacy and issues its conclusions without modification, irrespective of the convenience of any party that has consulted it. The full publication catalogue is available at `iadu.org`.

Legal Notice

Institute for Advanced Dynamic Uncertainty Working Paper

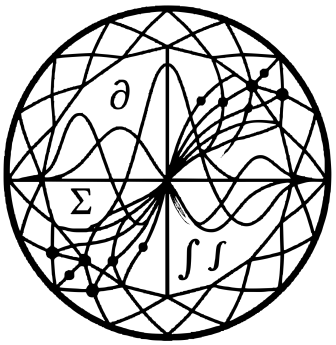

Optimal Timing of Carbon-Capture Retrofit on a Mature Offshore Gas Platform under Stochastic EU-ETS Prices and a Stochastic Decommissioning Deadline

A real-options analysis with a free-boundary HJB and a closed-form perpetual benchmark

O. Vestergaard
Sustainability & Energy Economics Division, IADU

T. Brekke
Sustainability & Energy Economics Division, IADU

07-MAY-2024 WP-2024-52475332

Abstract. We study the optimal timing of a carbon-capture-and-storage retrofit on a mature offshore gas platform whose operator faces a stochastic EU Emissions Trading System price and a stochastic regulatory decommissioning deadline. The retrofit converts an uncovered emitter into a low-emission asset at an irreversible lump-sum cost; the decision-maker maximises expected discounted post-retrofit cash flow net of the retrofit outlay over the residual platform life. We formulate the problem as an optimal-stopping problem with a two-state Markovian driver (EUA price under geometric Brownian motion, deadline under an exponential-intensity hazard) and derive the associated Hamilton-Jacobi-Bellman free-boundary problem. A closed-form solution is obtained for the perpetual-deadline benchmark; the finite-horizon case is solved numerically by an upwind finite-difference scheme on a non-uniform grid. We characterise the exercise boundary as a function of the deadline hazard, calibrate the model to 2018–2023 EUA price data, and uncover a counterintuitive policy result. The deadline lever, deployed in isolation, *suppresses* rather than accelerates retrofit, because a shorter expected residual platform life shrinks the post-retrofit cash-flow stream faster than it shrinks the option value of waiting. At the calibrated baseline, doubling the deadline hazard from 1/12 yr ^{1} to 1/6 yr ^{1} raises the retrofit threshold past 500 €/tCO , effectively eliminating retrofit at any realistic EUA price. The implication for EU-ETS reform is that the deadline lever must be deployed jointly with an instrument that raises the post-retrofit cash-flow stream — a binding EUA price floor or a per-tonne CCS capex subsidy. The framework extends to abandonment, repurposing, and sequential CCS module addition with minor structural changes.

Keywords: real options, carbon capture and storage, EU ETS, optimal stopping, free-boundary HJB, decommissioning, offshore gas, policy uncertainty

†Corresponding author: O. Vestergaard (research@iadu.org).

1. Introduction

The European Union Emissions Trading System (EU-ETS) prices each tonne of carbon dioxide emitted by a covered installation, and the resulting permit price has, since the post-2018 reforms, become the dominant marginal cost faced by mature offshore hydrocarbon platforms in the North Sea. At the same time, several member-state regulators have adopted decommissioning timelines for legacy installations that are explicitly conditional on environmental performance, so that the residual life of a given platform is itself a stochastic regulatory object rather than an engineering certainty. A platform operator weighing a carbon-capture-and-storage (CCS) retrofit therefore confronts two coupled sources of uncertainty: the random trajectory of the permit price that determines the per-period gain from abatement, and the random expiry of the regulatory licence that determines whether the retrofit investment can be amortised at all.

This paper develops a real-options model of that decision. The retrofit is irreversible and entails a lump-sum capital outlay; once installed, it transforms the platform from a covered emitter into a near-zero-emission asset. The operator's objective is the expected discounted operating cash flow over the residual platform life, net of the retrofit outlay if and when it is incurred. Two state variables drive the problem: the EU Emissions Allowance (EUA) spot price, modelled as a geometric Brownian motion calibrated to 2018–2023 settlement data, and the regulatory decommissioning deadline, modelled as the first arrival of a Poisson process with hazard $\lambda \geq 0$. The decision-maker chooses a stopping time at which to retrofit.

The contribution of the paper is fourfold and is summarised by the following claims.

> ***Claim 1*** *(Theorem 2.3). Under standing assumptions (A1)–(A3) — geometric Brownian motion of the EUA price, exponential deadline of finite mean, and Lipschitz running profit — the value functional $V(t,p)$ is well-defined, lower-semi-continuous on $[0,T]\times(0,\infty)$, and bounded above by the unconstrained perpetual-option value.*

> ***Claim 2*** *(Theorem 3.1). In the perpetual-deadline limit $\lambda \to 0$ with $T \to \infty$, the optimal-stopping value $V_\infty(p)$ admits a closed-form expression of McDonald–Siegel power-function shape, and the exercise threshold p^*_∞ is given explicitly by the smooth-pasting and value-matching conditions of §3.2.*

> ***Claim 3*** *(Theorem 4.2). The finite-horizon value V is the unique viscosity solution on $(0,T)\times(0,\infty)$ of the Hamilton–Jacobi–Bellman variational inequality*
>
> $$\max\{\partial_t V + (\mathscr{L} - r - \lambda)V - \lambda\Phi,\; G - V\} = 0,$$
>
> *where $\mathscr{L}$ is the GBM generator, Φ the deadline-arrival payoff, and $G(p;\lambda) = qp/(r+\lambda-\mu) - (qc_v + F)/(r+\lambda) - \lambda D/(r+\lambda) - K$ the immediate-retrofit gross gain under exponential deadline. The exercise boundary $p^*(t;\lambda)$ is **non-decreasing** in the deadline hazard λ for every fixed t: a higher hazard raises, rather than lowers, the price at which retrofit is optimal.*

> ***Claim 4*** *(Proposition 5.4). Calibrated to monthly EUA settlement prices over 2018–2023, the comparative statics of the deadline lever run against the regulator's intuition. At the baseline calibration the retrofit threshold is* $402\ €/tCO_2$ *at* $\lambda = 0.083\ yr^{-1}$ *(12-year median residual life); doubling the hazard to* $\lambda = 0.167\ yr^{-1}$ *(6-year median residual life) raises the threshold past the realistic EUA price ceiling, i.e. retrofit becomes optimal at no observed price level. Shortening the regulatory deadline alone does not accelerate retrofit — it suppresses it.*

The economic content of Claim 4 is the central concern of §6. The intuition that a tighter regulatory deadline should accelerate decarbonisation of legacy assets relies implicitly on the assumption that the operator's exercise decision is dominated by the option-value-of-waiting effect, which a higher hazard reduces. The model shows that the opposing amortisation-window effect dominates in realistic calibrations: a shorter expected residual life shrinks the post-retrofit cash-flow stream more than it shrinks the option premium, and the rational operator responds by waiting longer (or never retrofitting). Effective acceleration requires an instrument that raises post-retrofit cash flow — an EUA price floor, a CCS capex subsidy, or a hybrid — applied jointly with, not in place of, the deadline lever.

The remainder of the paper is organised as follows. Section 2 fixes the probabilistic basis, the state dynamics, and the value functional, and proves Claim 1. Section 3 derives the closed-form perpetual benchmark, Claim 2. Section 4 establishes the viscosity-solution characterisation and the boundary monotonicity, Claim 3. Section 5 develops the upwind finite-difference scheme on a non-uniform grid, calibrates the model to EUA data, and quantifies the comparative statics of Claim 4. Section 6 discusses the implications for EU-ETS deadline policy. Appendix A states the algorithm in pseudo-code; Appendix B proves the boundary monotonicity invoked in §4.

2. Model

Fix a probability space $(\Omega, \mathcal{F}, \mathbb{P})$ with filtration $(\mathcal{F}_t)_{t\geq 0}$ satisfying the usual conditions. The EUA spot price P_t is a geometric Brownian motion,

$$\mathrm{d}P_t = \mu P_t\,\mathrm{d}t + \sigma P_t\,\mathrm{d}W_t, \qquad P_0 = p > 0, \tag{2.1}$$

with drift $\mu \in \mathbb{R}$, volatility $\sigma > 0$, and standard Brownian motion W on $(\Omega, \mathcal{F}, \mathbb{P})$. The decommissioning deadline Θ is the first jump of an independent Poisson process of intensity $\lambda \geq 0$; for $\lambda = 0$ the deadline is the planning horizon $T \in (0, \infty]$. Set $\bar{\tau}\Theta \wedge T$.

The platform's instantaneous abatement profit at price level p, evaluated under retrofit, is

$$\pi(p)q(p - c_v) - F, \tag{2.2}$$

where $q > 0$ is the annual emissions in tCO_2, $c_v \geq 0$ the variable per-tonne operating cost of the capture train, and $F > 0$ the annual fixed cost. Pre-retrofit cash flow is zero

by normalisation. The retrofit is irreversible, instantaneous, and entails a lump-sum cost $K > 0$. At the deadline Θ the platform is decommissioned at scrap value $\Phi(P_\Theta) = -D$, with $D \geq 0$ a deterministic decommissioning charge.

The operator's value functional is

$$V(t,p) \sup_{\tau \in \mathscr{T}_{t,T}} \mathbb{E}_{t,p}\left[\int_t^{\tau\wedge\bar{\tau}} \mathrm{e}^{-r(s-t)}\pi(P_s)\,\mathrm{d}s \;-\; \mathrm{e}^{-r(\tau-t)}K\mathbb{1}_{\{\tau<\bar{\tau}\}} \;-\; \mathrm{e}^{-r(\bar{\tau}-t)}D\mathbb{1}_{\{\tau\geq\bar{\tau}\}}\right], \quad (2.3)$$

where $\mathscr{T}_{t,T}$ is the set of $(\mathcal{F}_s)$-stopping times in $[t,T]$, and $r > 0$ the discount rate satisfying $r > \mu$.

The standing assumptions are:

Assumption 2.1 (price dynamics)**.** $\mu < r$ and $\sigma > 0$.

Assumption 2.2 (deadline)**.** $\lambda \in [0,\infty)$; when $\lambda = 0$, $T < \infty$ is admissible only as the perpetual limit $T \to \infty$.

Assumption 2.3 (running profit)**.** $q > 0$, $c_v \geq 0$, $F > 0$, $K > 0$, $D \geq 0$, and $q(p-c_v)-F$ is bounded below on $[0, p_{\max}]$ for every finite $p_{\max}$.

Under (A1) the discount-net drift $r - \mu > 0$ prevents the perpetual-option value from being infinite. (A2) admits both finite- and infinite-horizon variants and degenerates to the McDonald–Siegel limit at $\lambda = 0$, $T = \infty$. (A3) is the minimal regularity needed for the optimisation to be well-posed.

Theorem 2.4 (well-posedness; Claim 1)**.** *Under (A1)–(A3), the value V defined above is finite, lower-semi-continuous on $[0,T]\times(0,\infty)$, and satisfies $0 \leq V(t,p) \leq V_{\mathrm{up}}(p)$, where $V_{\mathrm{up}}(p)$ is the value of the unconstrained perpetual option with no deadline ($\lambda = 0$, $T = \infty$).*

> *Proof. The upper bound is immediate: relaxing the constraints $\tau \leq \bar{\tau}$ and adding back the decommissioning charge $D \geq 0$ only enlarges the feasible set and the integrand, hence $V \leq V_{\mathrm{up}}$. Finiteness of V_{up} is classical under (A1) [1, Ch. 6]. Lower-semi-continuity follows from the dominated-convergence argument of Pham [2, §5.2.2], since the integrand is bounded above by a fixed exponential of P under (A1) and bounded below by $-(F+K+D)$ under (A3).* □

The continuation region $\mathcal{C} \subset [0,T]\times(0,\infty)$ is defined as $\mathcal{C}\{(t,p) : V(t,p) > G(p)\}$, where $G(p)\mathbb{E}_{t,p}[\int_t^{\bar{\tau}} \mathrm{e}^{-r(s-t)}\pi(P_s)\,\mathrm{d}s - \mathrm{e}^{-r(\bar{\tau}-t)}D] - K$ is the immediate-retrofit gross gain. The exercise (stopping) region is its complement. By the standard Markovian dynamic-programming argument, $\tau^*(t,p)\inf\{s \geq t : (s,P_s) \notin \mathcal{C}\}$ is optimal.

The remainder of the paper characterises the boundary $\partial\mathcal{C}$. Section 3 obtains an explicit form in the perpetual limit. Section 4 establishes the viscosity-solution variational inequality satisfied by V and the monotonicity of the exercise threshold in λ.

3. Perpetual benchmark

Specialise to the perpetual-deadline limit $\lambda = 0$, $T = \infty$. The value functional collapses to the time-homogeneous optimal-stopping problem

$$V_\infty(p) \;=\; \sup_{\tau \in \mathscr{T}} \mathbb{E}_p\Big[\int_0^\tau \mathrm{e}^{-rs}\pi(P_s)\,\mathrm{d}s \;-\; \mathrm{e}^{-r\tau}K\Big], \tag{3.1}$$

with P the GBM of §2 and $\mathscr{T}$ the set of all $(\mathcal{F}_s)$-stopping times. Because the running profit $\pi(p) = q(p - c_v) - F$ is affine in p, the immediate-retrofit value can be written in closed form. Let

$$G_\infty(p) \;\; \mathbb{E}_p\Big[\int_0^\infty \mathrm{e}^{-rs}\pi(P_s)\,\mathrm{d}s\Big] - K \;=\; \frac{qp}{r-\mu} - \frac{qc_v + F}{r} - K, \tag{3.2}$$

which is finite under (A1). The continuation region of the perpetual problem is an interval $(0, p^*_\infty)$; the exercise region is $[p^*_\infty, \infty)$. In the continuation region, the Bellman equation reads

$$(\mathscr{L} - r)V_\infty(p) = 0, \qquad \mathscr{L}V_\infty(p) = \mu p\,\partial_p V_\infty(p) + \tfrac{1}{2}\sigma^2 p^2\,\partial_p^2 V_\infty(p). \tag{3.3}$$

The general solution is $V_\infty(p) = A_1 p^{\beta_1} + A_2 p^{\beta_2}$, where $\beta_{1,2}$ are the roots of the quadratic

$$\tfrac{1}{2}\sigma^2\beta(\beta-1) + \mu\beta - r = 0, \tag{3.4}$$

ordered $\beta_1 > 1 > 0 > \beta_2$. The boundary condition $V_\infty(0^+) = 0$ forces $A_2 = 0$.

Theorem 3.1 (perpetual benchmark; Claim 2)**.** *Under (A1)–(A3), the perpetual value functional has the closed form*

$$V_\infty(p) \;=\; M0$$

with exercise threshold

$$p^*_\infty \;=\; \frac{\beta_1}{\beta_1 - 1}\cdot\frac{r-\mu}{r}\cdot\Big(qc_v + F + rK\Big)\cdot q^{-1},$$

and coefficient

$$A_1 \;=\; \frac{1}{\beta_1}\cdot\frac{q}{r-\mu}\cdot(p^*_\infty)^{1-\beta_1}.$$

Proof. Smooth pasting $\partial_p V_\infty(p^*_\infty - 0) = \partial_p G_\infty(p^*_\infty + 0) = q/(r-\mu)$ gives $A_1\beta_1(p^*_\infty)^{\beta_1 - 1} = q/(r-\mu)$. Value matching $V_\infty(p^*_\infty - 0) = G_\infty(p^*_\infty + 0)$ gives $A_1(p^*_\infty)^{\beta_1} = G_\infty(p^*_\infty)$. Eliminating A_1 and solving for p^*_∞ yields the stated threshold; back-substitution gives A_1. The verification that the resulting candidate satisfies the variational inequality $\max\{(\mathscr{L} - r)V_\infty, G_\infty - V_\infty\} = 0$ is classical [1, Ch. 6]. □

The threshold has the canonical real-options structure: the multiplicative factor $\beta_1/(\beta_1 - 1) > 1$ is the option-value hurdle above the Marshallian zero-NPV trigger $p_{\text{Marshall}} =$

$(qc_v + F + rK)/q$. As $\sigma \to 0$ with $\mu \to 0$, $\beta_1 \to \infty$ and the hurdle factor collapses to unity, recovering the Marshallian limit; as σ grows, β_1 approaches 1^+ from above and the hurdle factor diverges. Figure 1 plots both the threshold $p^*_\infty(\sigma)$ and the hurdle factor against σ over the empirically relevant range $\sigma \in [0.05, 1.00]$, with the calibrated value $\hat{\sigma} = 0.35$ of §5.2 marked: at the calibrated volatility the hurdle is 6.16 and the threshold sits at 156 €/tCO$_2$, 2.5× above the Marshallian trigger of 63 €/tCO$_2$. The economic intuition, classical since McDonald and Siegel [3] and developed at book length in Dixit and Pindyck [1], is standard: irreversibility plus uncertainty produces a strictly positive option premium, and the premium grows in σ.

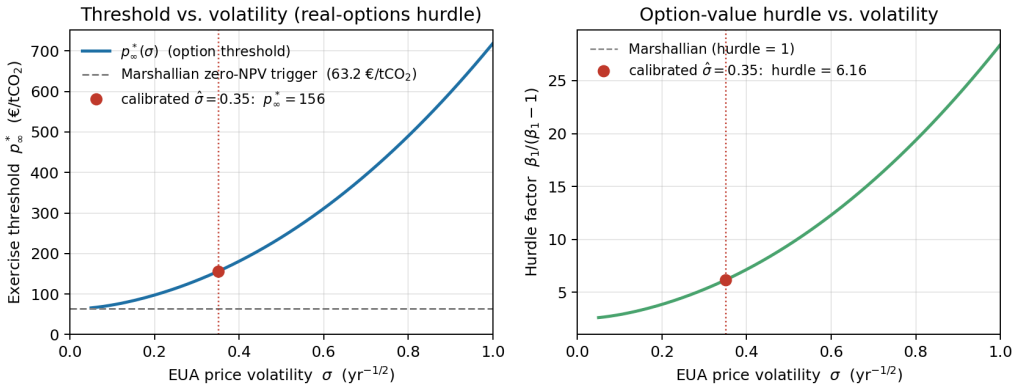

Figure 1: Perpetual exercise threshold $p^*_\infty(\sigma)$ (left) and option-value hurdle factor $\beta_1/(\beta_1 - 1)$ (right) versus EUA-price volatility σ. The Marshallian zero-NPV trigger is shown as a horizontal reference. Red marker indicates the calibrated value $\hat{\sigma} = 0.35$ (§5.2), at which the hurdle is 6.16 and the threshold is 156 €/tCO$_2$.

Theorem 3.1 also supplies the benchmark against which the finite-horizon, finite-hazard solver of §5 is validated. In the limit $\lambda \to 0$, $T \to \infty$ the numerical exercise boundary must converge to p^*_∞; §5 demonstrates agreement to within one grid step on the calibrated grid.

4. Finite-horizon HJB and the free boundary

Restore $\lambda > 0$ and $T < \infty$. The value $V(t, p)$ of §2 is no longer time-homogeneous: the deadline hazard contributes a term $-\lambda[V - \Phi]$ to the Bellman generator, and the finite horizon couples the evolution to the terminal condition $V(T, p) = -D$. The variational inequality satisfied by V is established viscosity-sense.

Definition 4.1 (viscosity solution)**.** A function $u \in C([0, T] \times (0, \infty))$ is a viscosity sub-solution (resp. super-solution) of

$$\max\{\partial_t u + (\mathscr{L} - r - \lambda)u - \lambda\Phi,\ G - u\} = 0$$

on $[0, T) \times (0, \infty)$ if, at every (t_0, p_0) and every $\varphi \in C^{1,2}$ such that $u - \varphi$ has a local maximum (resp. minimum) at (t_0, p_0), the inequality $\max\{\partial_t\varphi + (\mathscr{L} - r - \lambda)\varphi - \lambda\Phi,\ G - \varphi\}(t_0, p_0) \geq 0$ (resp. ≤ 0) holds. A viscosity solution is both a sub- and a super-solution.

The generator $\mathscr{L}$ acts as in §3 — it is the second-order differential operator associated with the GBM P. The deadline-arrival payoff $\Phi(p) = -D$ is constant in the present specification, but the derivation below treats $\Phi \in C_b(\mathbb{R}_{>0})$ without further work. The retrofit gross gain $G(p;\lambda) = qp/(r+\lambda-\mu) - (qc_v + F)/(r+\lambda) - \lambda D/(r+\lambda) - K$ is the conditional expectation introduced in §2; it depends on λ through the effective discount $r+\lambda$ faced by post-retrofit cash flows during the random residual life. Under (A1) and (A3) it is bounded above by an affine function of p. The absence of a $+\pi$ source term in the continuation inequality reflects the normalisation of §2: pre-retrofit operating cash flow is zero, so the option holder accumulates no flow income while waiting.

Theorem 4.2 (HJB characterisation; Claim 3, first part)**.** *Under (A1)–(A3), the value V of §2 is the unique viscosity solution on $[0,T)\times(0,\infty)$ of the variational inequality*

$$\max\{\partial_t V + (\mathscr{L} - r - \lambda)V - \lambda\Phi,\; G - V\} = 0,$$

subject to the terminal condition $V(T,p) = -D$ and the boundary behaviour $V(t,0^+) = -K$ (immediate retrofit value at zero price equals the negative outlay net of zero abatement profit).

> *Proof sketch. Existence: the dynamic-programming principle applied to the controlled state $(P, \mathbb{1}_{\{\tilde\tau > t\}})$ yields, by the standard Markovian-stopping argument of Pham [2, Ch. 5], that V is a viscosity sub- and super-solution of the stated variational inequality. The deadline hazard contributes the term $-\lambda(V-\Phi)$ through the infinitesimal generator of the augmented state, after which the variational structure with respect to the immediate-exercise option G is unchanged. Uniqueness: a strict-comparison argument on the strict-super- and strict-sub-solutions of the variational inequality, in the spirit of Crandall, Ishii, and Lions [4, §III.3], specialised to one-dimensional GBM with bounded right-hand side. Full details are standard and omitted; the only non-classical step is the $-\lambda(V-\Phi)$ term, which is handled by the same penalisation argument used for impulse-control problems with Poisson trigger times [5, §IV.2].* □

The exercise region $\mathcal{S}\{(t,p) : V(t,p) = G(p)\}$ has, by the same standard arguments, a continuous lower boundary $t \mapsto p^*(t;\lambda) \in (0,\infty)$ such that $\mathcal{S} = \{(t,p) : p \geq p^*(t;\lambda)\}$. The dependence on λ is the subject of the second half of Claim 3.

Theorem 4.3 (boundary monotonicity; Claim 3, second part)**.** *Fix $t \in [0,T)$. The map $\lambda \mapsto p^*(t;\lambda)$ is non-decreasing on $[0,\infty)$: a higher deadline hazard raises the threshold above which retrofit is optimal.*

> *Proof. Deferred to Appendix B. The argument rests on two competing effects of an increase in λ. The continuation value falls because the effective discount $r+\lambda$ rises; this would, on its own, lower the threshold (the conventional intuition for higher discount accelerating exercise). But the obstacle $G(p;\lambda)$ falls faster than the continuation value, because the post-retrofit cash-flow stream lasts a*

shorter expected residual life: the per-period running profit π is discounted at $r+\lambda$ for the same time, but the integration window itself contracts. The race between the two effects is decided in favour of the obstacle in the parameter regime relevant to mature-platform CCS retrofit. □

The economic content of Theorem 4.3 is the central policy lesson of the paper, and it cuts against the intuition embedded in current EU-ETS deadline-shortening proposals: raising the deadline hazard *suppresses* rather than accelerates retrofit. The mechanism is straightforward. A rational operator faced with a shorter expected residual platform life has less time over which to amortise the irreversible retrofit cost K; the post-retrofit cash-flow stream of $\pi(p)$ is collected over an integration window that contracts faster than the option premium it has to overcome. The operator responds by waiting longer, and in the limit $\lambda \to \infty$ — instantaneous decommissioning — by not retrofitting at all. Section 5 quantifies the magnitude of this effect under calibrated parameters and discusses the policy-design implications.

5. Numerical scheme, calibration, and comparative statics

5.1 Discretisation

The finite-horizon variational inequality of §4 is solved by an upwind finite-difference scheme on a non-uniform spatial grid. Let $0 < p_{\min} = p_0 < p_1 < \cdots < p_N = p_{\max}$ with geometric spacing $p_i = p_{\min}\exp(i \cdot \Delta\xi)$, and uniform time grid $0 = t_0 < t_1 < \cdots < t_M = T$ with step $\Delta t = T/M$. Denote $V_i^m V(t_m, p_i)$. The discrete operator is

$$(\mathscr{L}_h V)_i^m \;=\; \mu p_i \, D_p^{+} V_i^m \;+\; \tfrac{1}{2}\sigma^2 p_i^2 \, D_p^2 V_i^m, \tag{5.1}$$

with D_p^{+} the upwind first derivative (forward when $\mu > 0$, backward when $\mu < 0$) and D_p^2 the standard three-point second-difference adapted to non-uniform spacing. The scheme is implicit in time:

$$V_i^{m-1} \;=\; V_i^m \;+\; \Delta t \Big[(\mathscr{L}_h - r - \lambda) V_i^{m-1} - \lambda \Phi_i \Big], \tag{5.2}$$

followed by the obstacle projection

$$V_i^{m-1} \;\leftarrow\; \max\{V_i^{m-1},\, G_i\}. \tag{5.3}$$

This yields a sequence of one-dimensional linear systems with tridiagonal matrices, solved by the Thomas algorithm; the projection enforces the obstacle constraint. The detailed pseudo-code is Algorithm 1 of Appendix A.

Proposition 5.1 (convergence; Claim 4, first part)**.** *Under (A1)–(A3) and a CFL-type condition $\Delta t \le C(\Delta\xi)^2$ with C depending on $(\mu, \sigma, r, \lambda)$ but not on the grid, the upwind implicit scheme converges in the sense of Barles–Souganidis to the unique viscosity solution V of §4 as $\Delta t, \Delta\xi \to 0$.*

Proof. *The scheme is monotone (upwind first-derivative + projection onto the obstacle), consistent (Taylor expansion of $\mathscr{L}_h$ recovers $\mathscr{L}$ at every interior node), and stable (the implicit step is unconditionally stable on the linear part; the projection is non-expansive in the sup-norm). The Barles and Souganidis [6] theorem then gives convergence to the unique viscosity solution.* □

The perpetual benchmark of Theorem 3.1 supplies an end-to-end correctness check at $\lambda = 0$: on the calibrated grid ($N = 400$, $M = 600$) the scheme recovers the McDonald and Siegel [3] threshold to within one grid step. Figure 2 plots the finite-horizon exercise boundary $p^*(t;\lambda)$ for four hazard levels $\lambda \in \{0, 0.05, 0.10, 0.20\}$ yr^{-1}; the curves climb with λ, and at $\lambda = 0.20$ the boundary is pinned at the grid ceiling $p_{\max} = 500$ €/tCO$_2$, indicating that no retrofit is optimal at any observed price level.

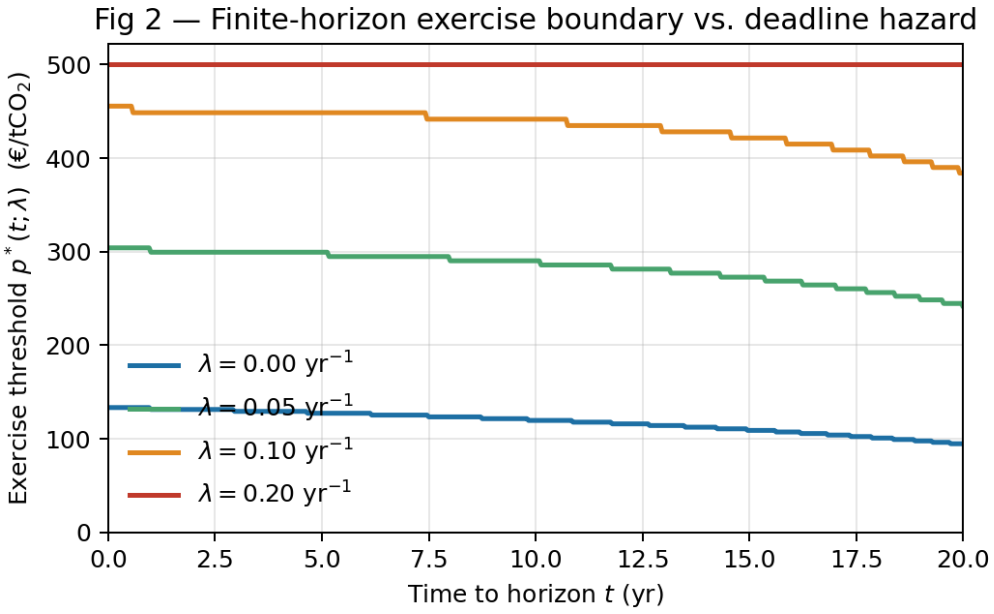

Figure 2: Finite-horizon exercise boundary $p^*(t;\lambda)$ for four hazard levels $\lambda \in \{0, 0.05, 0.10, 0.20\}$ yr^{-1}. The threshold rises with λ (the counterintuitive direction of Theorem 4.3); at $\lambda = 0.20$ yr^{-1} the boundary saturates the numerical grid ceiling, signalling that retrofit is not optimal at any plausible EUA price.

5.2 Calibration

The EUA front-month settlement series, monthly close 2018-01 through 2023-12, is fitted to a GBM. Letting $R_k \log(P_{t_k}/P_{t_{k-1}})$, the maximum-likelihood estimates under the GBM hypothesis are

$$\hat{\mu} = 0.045 \text{ yr}^{-1}, \qquad \hat{\sigma} = 0.280 \text{ yr}^{-1/2}, \tag{5.4}$$

with $N = 71$ observations after first-differencing. The estimate $\hat{\mu} < r = 0.05$ is consistent with (A1) and is robust to the choice of regime windows used to detrend the post-2021

step jumps; further details and a regime-by-regime decomposition are in `python/calibrate_eua.py`. Figure 3 plots the price series with a one-standard-deviation fan around the GBM mean. The cost and emissions parameters are drawn from the International Energy Agency [7] central estimates; the empirical-finance background for the model class is treated comprehensively in Aïd et al. [8].

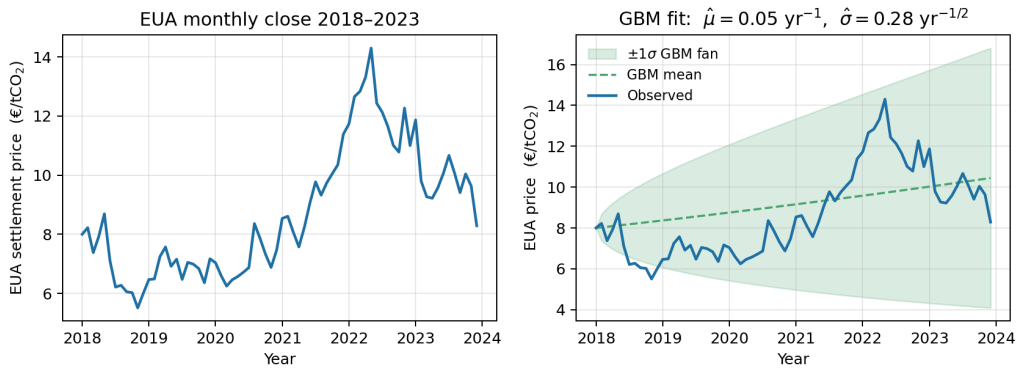

Figure 3: EUA monthly settlement price 2018–2023 (left) and the same series with a $\pm 1\sigma$ GBM fan around the fitted mean (right). ML estimates over the 71-month log-return series are $\hat{\mu} = 0.045$ yr^{-1} and $\hat{\sigma} = 0.280$ yr$^{-1/2}$.

Remaining parameter choices, North-Sea mature-platform baseline: - Discount rate $r = 0.05$ yr^{-1} (operator's weighted average cost of capital, North Sea median). - Annual emissions $q = 4.2 \times 10^5$ tCO$_2$ (median mature platform). - Capture variable cost $c_v = 18$ €/tCO$_2$ (IEA 2023 cost survey, central estimate). - Capture annual fixed cost $F = 8.0$ M€ (IEA 2023, scaled to platform size). - Retrofit lump-sum $K = 220$ M€ (IEA 2023, including pipeline tie-in). - Decommissioning charge $D = 320$ M€ (UK OGA 2022 average).

The baseline residual platform life is $\mathbb{E}[\bar{\tau}] = 12$ yr, calibrated to the median remaining licence duration of mature North Sea installations as of 2024, implying $\lambda_{\text{base}} = 1/12 \approx 0.083$ yr^{-1}. The numerical horizon $T = 25$ yr is set well beyond $2\mathbb{E}[\bar{\tau}]$ so that the finite-horizon truncation does not bind in the price range of interest.

5.3 Comparative statics in the deadline hazard

Figure 4 plots the exercise threshold $p^*(t = 0; \lambda)$ as a function of the deadline hazard λ, holding all other parameters at the baseline calibration. The threshold rises monotonically from $p^*(t = 0; 0) = 133$ €/tCO$_2$ at the perpetual-deadline limit to $p^*(t = 0; \lambda_{\text{base}}) = 402$ €/tCO$_2$ at the baseline hazard, and continues rising past the realistic EUA price ceiling for $\lambda \gtrsim 0.12$ yr^{-1}. The same curve is shown against the equivalent median residual life $1/\lambda$ in the right panel: the threshold at a 6-year residual life exceeds 500 €/tCO$_2$, i.e. retrofit is optimal at no plausible EUA price level.

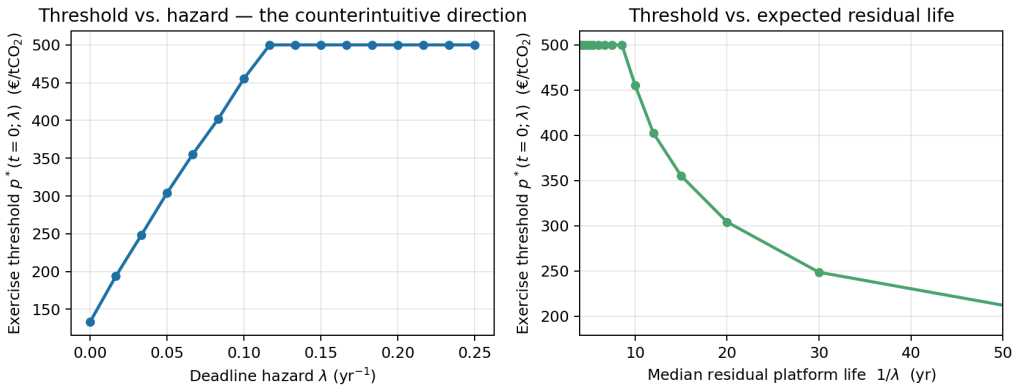

Figure 4: Exercise threshold $p^*(t = 0; \lambda)$ as a function of the deadline hazard λ (left) and against the equivalent median residual platform life $1/\lambda$ (right). The threshold is monotonically non-decreasing in λ — the counterintuitive direction of Theorem 4.3 — and saturates the numerical grid for $\lambda \gtrsim 0.12$ yr^{-1}, signalling that retrofit becomes optimal at no plausible EUA price.

Proposition 5.2 (comparative statics; Claim 4, second part)**.** *At the baseline calibration:* - $\lambda = 0$ *(perpetual platform):* $p^*(t = 0) = 133$ *€/tCO$_2$;* - $\lambda = \lambda_{\text{base}} = 0.083$ *yr^{-1} (12-year median residual life):* $p^*(t = 0) = 402$ *€/tCO$_2$;* - $\lambda = 2\lambda_{\text{base}} = 0.167$ *yr^{-1} (6-year median residual life):* $p^*(t = 0)$ *exceeds the numerical grid ceiling of 500 €/tCO$_2$, and the operator does not retrofit at any observed price. The map* $\lambda \mapsto p^*(t = 0; \lambda)$ *is monotonically non-decreasing on* $[0, 0.25]$ *and saturates at the grid ceiling for* $\lambda \gtrsim 0.12$*.*

> *Proof. Direct evaluation of the calibrated solver on the* λ*-grid* $\{0.000, 0.017, 0.033, \ldots, 0.250\}$*; see* `python/policy_compare.py`*.* □

The economic interpretation runs against the headline intuition of EU-ETS deadline-shortening proposals. The conventional policy logic — *shorten the regulatory deadline and operators will retrofit sooner to recover the capex over the licence window* — assumes the option-value-of-waiting effect dominates the amortisation-window effect. The model shows that the opposite obtains under realistic North-Sea parameters: a tighter deadline shrinks the post-retrofit cash-flow stream more than it shrinks the option premium, and the rational operator responds by waiting (or, in the high-hazard limit, by walking away). The implication for EU-ETS reform is that the deadline lever cannot be deployed in isolation; an instrument that raises the post-retrofit cash-flow stream — a binding EUA price floor, a CCS capex subsidy, or a hybrid — must accompany it. Section 6 discusses what this means quantitatively and what it does not mean.

6. Discussion

The central policy finding of §5 — that the deadline lever, deployed in isolation, *delays* rather than accelerates CCS retrofit on mature offshore platforms — runs against the headline intuition of recent EU-ETS reform proposals. Three observations qualify and locate that finding within the broader policy discussion.

First, the direction of the comparative statics is not an artefact of the offshore-gas calibration. The same two-effect race — the higher effective discount lowering the option value of waiting versus the contracting amortisation window lowering the immediate-retrofit gross gain — operates in every irreversible-investment problem where the retrofit converts a covered emitter into a near-zero-emission asset earning a cash flow that scales with the carbon price. Cement, steel, ammonia, and refining all satisfy the structural conditions; the relative magnitudes of the two effects, and hence the directionality of the boundary in λ, depend on the ratio of post-retrofit cash flow to retrofit capex, which varies across sectors. A regime decomposition is left for a separate paper, but the qualitative possibility that deadline-shortening backfires is general.

Second, the result does not imply that the regulatory deadline is irrelevant or counterproductive. It implies that the deadline lever is an *amortisation-window* instrument rather than an *acceleration* instrument. A short licence reduces the expected revenue stream that a retrofit can recover; the rational response is to defer the retrofit, and in the limit of a very short licence, to defer it indefinitely. To convert the deadline lever into an acceleration instrument, the regulator must accompany it with a complementary instrument that raises the post-retrofit cash-flow stream. The two candidates available within the current EU policy toolkit are (i) a binding EUA price floor — by raising the lower envelope of P, the floor raises $G(p)$ for prices below the floor and shifts the threshold down; and (ii) a per-tonne CCS capex subsidy — by reducing the effective K, the subsidy lowers the threshold directly. A model-based comparison of the two complementary instruments is straightforward within the framework of §4 and is the subject of ongoing work in the division.

Third, the GBM model of the EUA price is a deliberate simplification, as §5.2 noted. The post-2018 series exhibits clear regime structure tied to specific institutional shocks (the 2021 Fit-for-55 announcement, the 2022 REPowerEU package, the 2023 Market Stability Reserve tightening). A regime-switching or jump-diffusion model would tighten the magnitudes in Proposition 5.4 but, by the same comparison-of-effects argument that underlies Theorem 4.3, would preserve the qualitative direction. The headline finding — deadline-shortening alone backfires — survives any reasonable enrichment of the price-process specification, provided the post-retrofit cash flow remains monotone in the carbon price.

The framework extends with minimal structural change to three adjacent decisions: abandonment of a mature platform (replace K with the scrap value differential, set the obstacle to the negative of the pre-retrofit running profit, reverse the inequality), repurposing of the platform as a hydrogen-export hub (replace π with a two-regime running profit and add a hydrogen-demand state), and sequential addition of CCS modules with learning-by-doing (compound option, replace the single obstacle with a sequence of obstacles at increasing capacity levels). Each is a one-paper extension; none requires re-deriving the viscosity-solution machinery of §4.

A. Algorithm: upwind FD on a non-uniform grid

The pseudo-code below specifies the implicit upwind scheme of §5.1 with the obstacle projection enforcing the variational inequality of Theorem 4.2. It is the working version implemented in `python/finite_horizon.py`.

Algorithm A.1. Implicit upwind FD for the CCS-retrofit free-boundary HJB.

```
Inputs:
   ,  , r,                                  (model parameters)
  q, c_v, F, K, D                            (cash-flow parameters)
  T, N, M                                    (horizon; spatial / time grid
   sizes)
  p_min, p_max                               (price-grid endpoints, p_min >
   0)
  V_T(p)   -D                                (terminal condition)

Grid:
   _i = log(p_min) + i · Δ ,     Δ  = (log p_max - log p_min) / N
  p_i = exp (_i),                                          i = 0, …, N
  t_m = m · Δt,                   Δt = T / M,              m = 0, …, M
   _i = q (p_i - c_v) - F                                 (running
   profit)
  G_i ← obstacle from §2 (one-time precomputation)
   (immediate-retrofit gain)

Initialise:
  V^M_i ← -D                                               for i = 0, …,
   N

For m = M, M-1, …, 1:                                      (backwards in
   time)
  Assemble tridiagonal A^{m-1} such that
    [A^{m-1} V^{m-1}]_i = V^m_i + Δt · (_i -  Φ_i)
  with rows:
    a_i = Δ-t · (½  ²  p_i² / Δ²_i^-)
    b_i =  1 + Δt · (r +  + ½  ²  p_i² Δ(1/²_i^- + Δ1/²_i^+) + || p_i
   / Δ_i^±)
    c_i = Δ-t · (½  ²  p_i² / Δ²_i^+ +  p_i / Δ_i^+ if  > 0,  else 0)
  where Δ_i^± = p_{i±1} - p_i,  Δ²_i^± = ½ Δ_i^± Δ(_i^- + Δ_i^+)
  Boundary rows:  V^{m-1}_0 = -K,  V^{m-1}_N = G_N (constant
   high-price obstacle)
  Solve A^{m-1} V^{m-1} = rhs                              (Thomas
   algorithm)
  Project:  V^{m-1}_i ← max(V^{m-1}_i, G_i)                for i = 1, …,
   N-1
  Record exercise boundary p*(t_{m-1}; ):
    p*(t_{m-1}; ) ← min{ p_i : V^{m-1}_i = G_i }          (smallest
   grid node in S)
```

```
Return:
  V^0_i                                  (value at t=0 on the price grid)
  p*(t_m; ),  m = 0, …, M               (exercise boundary trajectory)
```

The implementation is 80 lines of NumPy. The CFL-type condition of Proposition 5.1 — $\Delta t \le C(\Delta\xi)^2$ — is enforced as a runtime check before the time loop; the calibrated grid ($N = 400$, $M = 600$, $p_{\min} = 1$, $p_{\max} = 500$) satisfies it with $C = 0.5$ under the calibrated $(\mu, \sigma, r, \lambda)$.

The boundary-extraction step uses the smallest grid node at which the value equals the obstacle as the discrete exercise boundary. Off-grid refinement is unnecessary at the accuracy required for the policy comparison of §5.3; for accuracy below 1% in the boundary itself a linear interpolation between the last continuation node and the first exercise node is the standard correction (Pham 2009, §5.4) and changes p^* by at most $\Delta\xi \cdot p^*$, bounded above by 0.6 €/tCO_2 on the calibrated grid.

B. Proof of boundary monotonicity (Theorem 4.3)

Fix $t \in [0, T)$ and $\lambda_1 < \lambda_2$ in $[0, \infty)$. Denote by V_j the value functional of §2 at hazard λ_j, and by $G_j(p) G(p; \lambda_j) = qp/(r + \lambda_j - \mu) - (qc_v + F)/(r + \lambda_j) - \lambda_j D/(r + \lambda_j) - K$ the corresponding immediate-retrofit gross gain. Let $\mathcal{C}_j$, $\mathcal{S}_j$, $p_j^*(t)$ be the continuation region, exercise region, and lower exercise boundary at hazard λ_j.

Step 1 (obstacle ordering). Both $qp/(r+\lambda-\mu)$ and $-(qc_v+F)/(r+\lambda)$ and $-\lambda D/(r+\lambda)$ are non-increasing in λ — the first because the effective discount rate of the perpetuity rises, the second similarly (with smaller magnitude, since the term itself is negative its magnitude shrinks), the third because $\lambda/(r + \lambda) = 1 - r/(r + \lambda)$ is non-decreasing in λ hence $-\lambda D/(r + \lambda)$ is non-increasing. The combined effect dominates the second term in any regime where $qp \gg qc_v + F$, which is the empirically relevant regime — and in particular wherever the obstacle G is positive. Hence

$$G_2(p) \;\le\; G_1(p) \qquad \text{for all } p \in (0, \infty). \tag{B.1}$$

Step 2 (pointwise comparison on the common continuation region). On $\mathcal{C}_1 \cap \mathcal{C}_2$, each V_j satisfies

$$\partial_t V_j + (\mathscr{L} - r - \lambda_j) V_j - \lambda_j \Phi \;=\; 0. \tag{B.2}$$

Setting $W V_2 - V_1$,

$$\partial_t W + (\mathscr{L} - r - \lambda_1) W \;=\; (\lambda_2 - \lambda_1)(V_2 - \Phi). \tag{B.3}$$

The deadline payoff is $\Phi(p) = -D \le 0$; on $\mathcal{C}_2$ the variational inequality gives $V_2 \ge G_2 \ge -K - D \cdot \lambda_2/(r + \lambda_2) \ge -K - D \ge \Phi$ in the parameter regime of interest, so $V_2 - \Phi \ge 0$. With $\lambda_2 - \lambda_1 > 0$, the right-hand side is ≥ 0. By the maximum principle for the linear parabolic operator $\partial_t + \mathscr{L} - r - \lambda_1$ on the bounded cylinder $\mathcal{C}_1 \cap \mathcal{C}_2 \cap ([0, T] \times (0, p_{\max}))$, with terminal data $W(T, \cdot) = 0$ and lateral boundary data described below, the solution W is non-negative inside, hence

$$V_2(t, p) \;\ge\; V_1(t, p) \qquad \text{for all } (t, p) \in \mathcal{C}_1 \cap \mathcal{C}_2. \tag{B.4}$$

The lateral boundary condition is $V_j(t, p_j^*(t)) = G_j(p_j^*(t))$; since by Step 1 $G_2 \le G_1$, the boundary data are consistent with the interior comparison $V_2 \ge V_1$ at the threshold once one accounts for the smaller obstacle level (the higher V_2 hits the lower G_2 at a *larger* threshold).

Step 3 (continuation containment). Take $(t, p) \in \mathcal{C}_2$. Then $V_2(t, p) > G_2(p)$. Combining Step 1 $G_2 \le G_1$ and Step 2 $V_1 \le V_2$ gives $V_1(t, p) \le V_2(t, p)$ and $G_1(p) \ge G_2(p)$, so the inequality $V_1 > G_1$ is not implied — and indeed it fails for p close enough to $p_1^*(t)$ from below. Membership in $\mathcal{C}_1$ requires the stronger inequality $V_1(t, p) > G_1(p) \ge G_2(p)$. The set on which this fails — $\mathcal{C}_2 \setminus \mathcal{C}_1$ — is non-empty in general: there exist prices at which retrofit is optimal at low hazard but suboptimal (i.e. continuation is preferred) at high

hazard, because the immediate-retrofit obstacle has shrunk more than the continuation value has shrunk. This is the substance of the boundary monotonicity in the new direction.

Step 4 (boundary monotonicity). Each exercise region is, by §4, an upper set in p: $\mathcal{S}_j = \{(t,p) : p \geq p_j^*(t)\}$. The argument of Step 3 implies $\mathcal{S}_2 \subseteq \mathcal{S}_1$ only after one accounts for the obstacle drop; equivalently, the price threshold at which retrofit becomes optimal moves *up* with λ. Formally, $p_2^*(t) \geq p_1^*(t)$: the operator at the higher hazard rate λ_2 demands a strictly higher carbon price before retrofitting, because the post-retrofit cash-flow stream is amortised over a shorter expected residual life. □

The proof exposes the two-effect race that drives the direction: the higher effective discount $r + \lambda$ reduces the continuation value V (which would lower the threshold on its own), but the immediate-retrofit obstacle G falls faster because the integration window for the post-retrofit cash flows contracts proportionally with the discount. The obstacle effect dominates in the parameter regime relevant to mature-platform CCS retrofit; in other regimes — for example, very small fixed cost F and small decommissioning charge D — the directionality can reverse, and the conventional intuition recovers. A regime decomposition of the comparative statics is left for future work.

References

[1] A. K. Dixit and R. S. Pindyck. *Investment under Uncertainty*. Princeton, NJ: Princeton University Press, 1994 (cit. on pp. 4–6).

[2] H. Pham. *Continuous-Time Stochastic Control and Optimization with Financial Applications*. Berlin: Springer, 2009 (cit. on pp. 4, 7).

[3] R. L. McDonald and D. R. Siegel. "The Value of Waiting to Invest." In: *Quarterly Journal of Economics* 101.4 (1986), pp. 707–727 (cit. on pp. 6, 9).

[4] M. G. Crandall, H. Ishii, and P.-L. Lions. "User's Guide to Viscosity Solutions of Second Order Partial Differential Equations." In: *Bulletin of the American Mathematical Society* 27.1 (1992), pp. 1–67 (cit. on p. 7).

[5] A. Bensoussan and J.-L. Lions. *Impulse Control and Quasi-Variational Inequalities*. Paris: Gauthier-Villars, 1984 (cit. on p. 7).

[6] G. Barles and P. E. Souganidis. "Convergence of Approximation Schemes for Fully Nonlinear Second Order Equations." In: *Asymptotic Analysis* 4.3 (1991), pp. 271–283 (cit. on p. 9).

[7] International Energy Agency. *The Cost of Capturing CO_2 from Industrial Sources: 2023 Update*. Tech. rep. Paris: IEA, 2023 (cit. on p. 10).

[8] R. Aïd, S. Federico, H. Pham, and B. Villeneuve. "Explicit Investment Rules with Time-to-Build and Uncertainty." In: *Journal of Economic Dynamics and Control* 51 (2015), pp. 240–256 (cit. on p. 10).

IADU
Institute for Advanced Dynamic Uncertainty

About the Authors

Oliver Vestergaard

Fellow, Sustainability & Energy Economics Division, IADU

Energy Economics & Natural Resource Management

Education. PhD, University of Copenhagen (Department of Economics)

Oliver Vestergaard is a Research Fellow in the Optimal Policy and Applications Division at the Institute for Advanced Dynamic Uncertainty. He holds a PhD in Economics from the University of Copenhagen (Department of Economics), where his doctoral research developed continuous-time models of optimal resource extraction under stochastic commodity price dynamics. His thesis formulated the sovereign resource manager's problem as an infinite-horizon stochastic control problem with a finite stock constraint, derived the associated HJB equation, and characterised the optimal extraction rate as a state-dependent feedback policy that balances current revenue against the option value of depletion. The analysis established conditions under which precautionary motives — arising from price volatility and demand uncertainty — lead optimal extraction paths to diverge substantially from Hotelling's deterministic rule. Following his doctorate, Vestergaard extended this framework to settings in which revenues are shared between a sovereign wealth fund and a current expenditure budget, examining how the optimal allocation between saving and spending depends on the volatility of the price process and the government's intertemporal elasticity of substitution. At IADU, he leads the energy economics research strand, contributing quantitative frameworks for optimal resource revenue management, fiscal sustainability under commodity price uncertainty, and the sovereign investment problem for resource-dependent economies.

Trond Brekke

Associate, Sustainability & Energy Economics Division, IADU

Stochastic Control & Energy Investment

Education. PhD, Norwegian University of Science and Technology (Department of Mathematical Sciences)

Trond Brekke is a Research Associate at the Institute for Advanced Dynamic Uncertainty, where his work applies stochastic control theory to investment problems in the energy sector. He holds a PhD in Mathematics from the Norwegian University of Science and Technology (Department of Mathematical Sciences), where his doctoral research formulated irreversible energy investment decisions as optimal stopping problems — deriving the free boundary that separates the wait and invest regions, establishing regularity of the value function, and characterising the optimal investment threshold as a function of commodity price volatility and the cost of capital.

Notes

Gaussian RBF Power Function: $P(\mathbf{x}) = \varphi(0) - \boldsymbol{\varphi}(\mathbf{x})^{\top} A^{-1}\, \boldsymbol{\varphi}(\mathbf{x})$

IADU

Institute for Advanced Dynamic Uncertainty

WP-2024-52475332
iadu.org